

# Effective-Lagrangian approach to $\gamma\gamma \rightarrow WW$ ; I: Couplings and amplitudes

O. NACHTMANN<sup>1</sup>, F. NAGEL<sup>2</sup>, M. POSPISCHIL<sup>3</sup> AND A. UTERMANN<sup>4</sup>

*Institut für Theoretische Physik, Philosophenweg 16, D-69120 Heidelberg, Germany*

## Abstract

We consider the gauge-boson sector of a locally  $SU(2) \times U(1)$  invariant effective Lagrangian with ten dimension-six operators added to the Lagrangian of the Standard Model. These operators induce anomalous three- and four-gauge-boson couplings and an anomalous  $\gamma\gamma H$  coupling. In the framework of this effective Lagrangian we calculate the helicity amplitudes and differential and total cross sections for the process  $\gamma\gamma \rightarrow WW$  at a photon collider. We give relations between different parts of the amplitudes that show which linear combinations of anomalous couplings are measurable in this reaction. The transformation properties of the differential cross section under  $CP$  are discussed. We find that three linear combinations of  $CP$  conserving and of  $CP$  violating couplings can be measured independently of the photon polarisation in  $\gamma\gamma \rightarrow WW$ .

---

<sup>1</sup>email: O.Nachtmann@thphys.uni-heidelberg.de

<sup>2</sup>email: F.Nagel@thphys.uni-heidelberg.de

<sup>3</sup>Now at CNRS UPR 2191, 1 Avenue de la Terrasse, F-91198 Gif-sur-Yvette, France,  
email: Martin.Pospischil@iaf.cnrs-gif.fr

<sup>4</sup>email: A.Utermann@thphys.uni-heidelberg.de

# Contents

1	Introduction	3
2	Cross section for $\gamma\gamma \rightarrow WW \rightarrow 4$ fermions	5
3	$CP$ symmetry	13
4	Conclusions	16
A	Effective Lagrangian	17
B	Feynman rules	19
C	Particle momenta and polarisations	23
D	Helicity amplitudes	23

# 1 Introduction

Given the large variety of particle-physics models that claim to replace the Standard Model (SM) at a high energy scale  $\Lambda$ , it is a vital approach for precision experiments at a future  $e^+e^-$  linear collider ILC with a design like TESLA [1] or CLIC [2] to probe new-physics effects in a model-independent way. A  $\gamma\gamma$  collider—where two high-energy photons are obtained through Compton backscattering off high-energy electrons— extends the physics potential of an ILC substantially. Such a photon-collider option is planned for example at  $e^+e^-$  machines like TESLA [3] or CLIC [4]. The SM is very successful at energies up to the electroweak scale, set by the vacuum expectation value,  $v \approx 246$  GeV, of the SM-Higgs-boson field. Assuming

$$\Lambda \gg v \tag{1.1}$$

the new-physics effects can be taken into account using an effective Lagrangian that consists of the SM Lagrangian supplemented by operators of dimension higher than four, see [5,6] and references therein. We adopt the approach of [5], where all operators up to dimension six are constructed that contain only SM fields and are invariant under the SM gauge symmetry  $SU(3) \times SU(2) \times U(1)$ . In a preceding work [7] we have extensively discussed the gauge-boson sector of such a Lagrangian,

$$\mathcal{L}_{\text{eff}} = \mathcal{L}_0 + \mathcal{L}_2, \tag{1.2}$$

where  $\mathcal{L}_0$  is the Lagrangian of the SM (for our conventions see App. A) and the second term

$$\begin{aligned} \mathcal{L}_2 = & \left( h_W O_W + h_{\tilde{W}} O_{\tilde{W}} + h_{\varphi W} O_{\varphi W} + h_{\varphi \tilde{W}} O_{\varphi \tilde{W}} + h_{\varphi B} O_{\varphi B} + h_{\varphi \tilde{B}} O_{\varphi \tilde{B}} \right. \\ & \left. + h_{WB} O_{WB} + h_{\tilde{W}B} O_{\tilde{W}B} + h_{\varphi}^{(1)} O_{\varphi}^{(1)} + h_{\varphi}^{(3)} O_{\varphi}^{(3)} \right) / v^2, \end{aligned} \tag{1.3}$$

contains all dimension-six operators that either consist only of electroweak gauge-boson fields or that contain both gauge-boson fields and the SM-Higgs field. There is no gauge invariant dimension-five operator that can be constructed out of these fields. We list the definitions of the operators of  $\mathcal{L}_2$  in App. A. Four operators are  $CP$  violating, namely those containing the dual  $W$ - or  $B$ -field strengths; they are denoted by a tilde on the subscripts in (1.3). We have divided by  $v^2$  in order to render the coupling constants  $h_i$  dimensionless. The  $h_i$  are subsequently called anomalous couplings. We have

$$h_i \sim O(v^2/\Lambda^2). \tag{1.4}$$

The new operators (1.3) have an impact on a large number of electroweak precision observables as calculated in [6–8]. It is particularly interesting to study the rich phenomenology induced by the Lagrangian (1.2) at an ILC both in the high-energy  $e^+e^-$  and  $\gamma\gamma$  modes, and in the Giga- $Z$  mode.

There are other ways to parametrise new-physics effects. For instance in a form-factor approach for the  $\gamma WW$  and  $ZWW$  couplings anomalous effects are parametrised by 28 real parameters if one also allows for imaginary parts in the form factors [9]. In such a framework no anomalous contributions at the fermion-boson vertices or at the boson propagators occur. The sensitivity to the anomalous triple-gauge-boson couplings in the reaction  $e^+e^- \rightarrow WW$  at an ILC for different beam polarisations has been studied in detail in [10]. There are ways to translate the bounds on the anomalous couplings from the form-factor approach to the effective-Lagrangian approach [7]. In the same reference also the advantages of the different approaches are surveyed and a discussion of the relation to other work on anomalous electroweak gauge-boson couplings in  $e^+e^-$  annihilation [1, 9–17] is given.

In the form-factor approach implications from a future  $\gamma\gamma$  collider for anomalous couplings were discussed in [17–25]. At tree level anomalous triple gauge-boson couplings from the  $\gamma WW$  vertex but not from the  $ZWW$  vertex contribute. In [17] it was argued that the precision for the measurement of the  $\gamma WW$  coupling is comparable in the  $e^+e^-$  and the  $\gamma\gamma$  modes. The  $\gamma\gamma WW$  vertex contributes already at tree level at a photon collider. Hence also implications from anomalous quartic gauge-boson couplings can be investigated. Certain analyses of anomalous couplings at a  $\gamma\gamma$  collider are focused on anomalous triple gauge-boson couplings [17, 18], on anomalous quartic gauge-boson couplings [19, 20] and on  $CP$ -violating gauge-boson couplings [21, 26]. In [22–24] the finite width of the  $W$  boson and virtual and real corrections [24] are also taken into account. For a discussion of the anomalous  $\gamma\gamma H$  vertex in the  $\gamma\gamma$  and  $e\gamma$  modes at an ILC see [25]. Implications for the process  $\gamma\gamma \rightarrow WW$  induced by some of the dimension-six operators in (1.3) were investigated in [26, 27].

In our present work we study, in the framework of the Lagrangian (1.2), the process  $\gamma\gamma \rightarrow WW \rightarrow 4$  fermions. In the reaction  $\gamma\gamma \rightarrow WW$  anomalous contributions to the  $\gamma WW$ ,  $\gamma\gamma WW$  and  $\gamma\gamma H$  vertices can be studied. We do this by applying the Lagrangian (1.2) and (1.3) as calculated in [7] in terms of the physical fields  $A$ ,  $Z$ ,  $W^\pm$  and  $H$ . Finally we expand to linear order in the anomalous couplings. Throughout this and the companion paper II [28], we use the parameter scheme  $P_W$  (see Sect. 4.2 of [7]), which contains the  $W$  boson mass  $m_W$  as an input parameter. In Sect. 4.1 of [7] we discussed the scheme  $P_Z$ , which contains the  $Z$  boson mass  $m_Z$  as an input parameter. There the  $h_i$  would modify the  $W$  mass and therefore the kinematics of the reaction, which is highly inconvenient. Let us mention that in our approach, where we use the effective Lagrangian (1.2) to construct all required interactions, no further assumptions are needed to relate the cross sections for the  $e^+e^-$  and the  $\gamma\gamma$  modes. On the other hand in the form-factor approach one has to add for every contributing vertex new form factors. Hence it is getting more involved to calculate combined constraints from the  $e^+e^-$  and the  $\gamma\gamma$  modes on anomalous couplings. In the companion paper [28] we will compare the sensitivity on the couplings in (1.3) from the  $e^+e^-$  and  $\gamma\gamma$  modes and high precision observables. To this end we shall calculate in [28] the minimum errors on the anomalous couplings obtainable in  $\gamma\gamma \rightarrow WW$  by

means of optimal observables [11, 29].

Our paper is organised as follows: In Sect. 2 we derive the helicity amplitudes and the differential cross section for the process  $\gamma\gamma \rightarrow WW$  with fixed c.m. energy. In Sect. 3 the discrete-symmetry properties of the anomalous interactions are explained. We present our conclusions in Sect. 4. In App. A we give our conventions for the SM Lagrangian and list the additional dimension-six operators of the effective Lagrangian. Those Feynman rules derived from the effective Lagrangian that are needed for the calculation of the process  $\gamma\gamma \rightarrow WW \rightarrow 4$  fermions are listed in App. B. In App. C we give our conventions for particle momenta and polarisation vectors. The analytic results for the helicity amplitudes of the production process  $\gamma\gamma \rightarrow WW$  are given in App. D.

## 2 Cross section for $\gamma\gamma \rightarrow WW \rightarrow 4$ fermions

In this section we derive the spin-averaged differential cross section for the process

$$\gamma\gamma \rightarrow W^-W^+ \rightarrow (f_1\bar{f}_2)(f_3\bar{f}_4) \quad (2.1)$$

in the scheme  $P_W$ . The final-state fermions in (2.1) are leptons or quarks. We consider this reaction for fixed photon energies in the framework of the effective Lagrangian (1.2). The case where the initial photons are not monochromatic but have Compton energy-spectra raises additional complications with the kinematical reconstruction of the final state. This will be considered in [28] applying the methods presented in [30]. Our notation for particle momenta and helicities is shown in Fig. 1. The production of the  $W$  bosons is described in the  $\gamma\gamma$  c.m. frame. Our coordinate

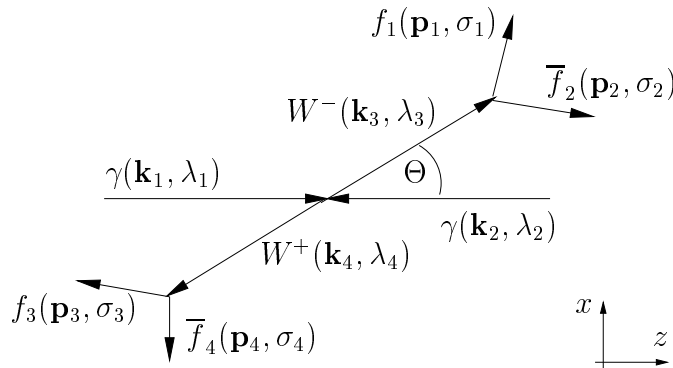


Figure 1: Conventions for particle momenta and helicities.

axes are chosen such that the  $WW$ -boson production takes place in the  $x$ - $z$  plane, the photon momentum  $\mathbf{k}_1$  points in the positive  $z$ -direction and the  $y$  unit vector is given by  $\hat{\mathbf{e}}_y = (\mathbf{k}_1 \times \mathbf{k}_3)/|\mathbf{k}_1 \times \mathbf{k}_3|$ . In the  $\gamma\gamma$  c.m. frame and at a given c.m. energy

$\sqrt{s}$ , a pure initial state of two photons is uniquely specified by the photon helicities:

$$|\lambda_1 \lambda_2\rangle = |\gamma(\mathbf{k}_1, \lambda_1) \gamma(\mathbf{k}_2, \lambda_2)\rangle \quad (\lambda_1, \lambda_2 = \pm 1). \quad (2.2)$$

Then the differential cross section for an unpolarised initial state is

$$d\sigma = \frac{1}{2s} \frac{1}{4} \sum_{\lambda_1, \lambda_2} |\langle f | \mathcal{T} | \lambda_1 \lambda_2 \rangle|^2 d\Gamma, \quad (2.3)$$

where  $\mathcal{T}$  is the transition operator,  $|f\rangle = |f_1(\mathbf{p}_1, \sigma_1) \bar{f}_2(\mathbf{p}_2, \sigma_2) f_3(\mathbf{p}_3, \sigma_3) \bar{f}_4(\mathbf{p}_4, \sigma_4)\rangle$  is the final state and the phase-space measure for final states is as usual

$$d\Gamma = \left( \prod_{i=1}^4 \frac{d^3 p_i}{(2\pi)^3 2p_i^0} \right) (2\pi)^4 \delta^{(4)} \left( k_1 + k_2 - \sum_{i=1}^4 p_i \right). \quad (2.4)$$

Using the narrow-width approximation for the  $W$  bosons and considering all final-state fermions to be massless, we obtain

$$\frac{d\sigma}{d\cos\Theta d\cos\vartheta d\varphi d\cos\bar{\vartheta} d\bar{\varphi}} = \frac{3\beta}{2^{13}\pi^3 s} B_{12} B_{34} \mathcal{P}_{\lambda'_3 \lambda'_4}^{\lambda_3 \lambda_4} \mathcal{D}_{\lambda'_3}^{\lambda_3} \bar{\mathcal{D}}_{\lambda'_4}^{\lambda_4}, \quad (2.5)$$

where summation over repeated indices is implied and  $\beta = (1 - 4m_W^2/s)^{1/2}$  is the velocity of each  $W$  boson in the  $\gamma\gamma$  c.m. frame. The branching ratio for the decay  $W \rightarrow f_i \bar{f}_j$  is denoted by  $B_{ij}$ . The  $W$  helicity states are defined in the coordinate system shown in Fig. 1. For the definition of the polarisation vectors see App. C. The polar angle between the positive  $z$ -axis and the  $W^-$  momentum is denoted by  $\Theta$ . The cross section does not depend on the azimuthal angle of the  $W^-$  momentum due to rotational invariance. The respective frames for the decay tensors are defined by a rotation by  $\Theta$  about the  $y$ -axis of the frame in Fig. 1 such that the  $W^-$  ( $W^+$ ) momentum points in the new positive (negative)  $z$ -direction and a subsequent rotation-free boost into the c.m. system of the corresponding  $W$  boson. The spherical coordinates  $\vartheta, \varphi$  and  $\bar{\vartheta}, \bar{\varphi}$  are those of the  $f_1$ - and  $\bar{f}_4$ -momentum directions, respectively. The production and decay tensors in (2.5) are given by

$$\mathcal{P}_{\lambda'_3 \lambda'_4}^{\lambda_3 \lambda_4}(\Theta) = \sum_{\lambda_1, \lambda_2} \mathcal{M}(\lambda_1, \lambda_2; \lambda_3, \lambda_4) \mathcal{M}^*(\lambda_1, \lambda_2; \lambda'_3, \lambda'_4), \quad (2.6)$$

$$\mathcal{M}(\lambda_1, \lambda_2; \lambda_3, \lambda_4) \equiv \langle W^-(\mathbf{k}_3, \lambda_3) W^+(\mathbf{k}_4, \lambda_4) | \mathcal{T} | \gamma(\mathbf{k}_1, \lambda_1) \gamma(\mathbf{k}_2, \lambda_2) \rangle, \quad (2.7)$$

$$\mathcal{D}_{\lambda'_3}^{\lambda_3}(\vartheta, \varphi) = l_{\lambda_3} l_{\lambda'_3}^*, \quad (2.8)$$

$$\bar{\mathcal{D}}_{\lambda'_4}^{\lambda_4}(\bar{\vartheta}, \bar{\varphi}) = \bar{l}_{\lambda_4} \bar{l}_{\lambda'_4}^*, \quad (2.9)$$

where we have suppressed the phase-space variables on the right hand side. The functions occurring in the decay tensors are listed in App. D.

	SM	$h_W$	$h_{\tilde{W}}$	$h_{\varphi W}$	$h_{\varphi \tilde{W}}$	$h_{\varphi B}$	$h_{\varphi \tilde{B}}$	$h_{WB}$	$h_{\tilde{W}B}$	$h_\varphi^{(1)}$	$h_\varphi^{(3)}$
$\gamma WW$	✓	✓	✓					✓	✓		
$ZWW$	✓	✓	✓					✓	✓		$P_Z$
$\gamma\gamma WW$	✓	✓	✓								
$\gamma\gamma H$				✓	✓	✓	✓	✓	✓		

Table 1: Contributions of the SM Lagrangian and of the anomalous operators (1.3) to different vertices in order  $O(h)$ . The coupling  $h_\varphi^{(3)}$  contributes to the  $ZWW$  vertex in the scheme  $P_Z$  but not in  $P_W$ .

To first order in the anomalous couplings the production amplitude  $\mathcal{M}$  contains the SM diagrams (Fig. 2), diagrams containing one anomalous triple- or quartic-gauge-boson vertex (Fig. 3), and an  $s$ -channel Higgs-boson exchange (Fig. 4). The Feynman rules that are necessary to compute these diagrams are listed in App. B. Tab. 1 shows which operators contribute to the three kinds of anomalous vertices in Figs. 3 and 4. We expand the production amplitudes to first order in the anomalous couplings:

$$\mathcal{M} = \mathcal{M}_{\text{SM}} + \sum_i h_i \mathcal{M}_i + O(h^2), \quad (2.10)$$

where all particle momenta and helicities are suppressed.  $\mathcal{M}_{\text{SM}}$  is the SM tree-level amplitude and  $i = W, \tilde{W}, \varphi W, \varphi \tilde{W}, \varphi B, \varphi \tilde{B}, WB, \tilde{W}B$ . The couplings  $h_\varphi^{(1)}$  and  $h_\varphi^{(3)}$  do not enter the amplitudes (2.10) to first order. The different terms on the right hand side of (2.10) for the various helicity combinations of the incoming and outgoing gauge bosons are listed in App. D. We find relations between amplitudes corresponding to different anomalous couplings. These relations depend on combinations of input parameters of  $P_W$ ,

$$s_1^2 \equiv \frac{e^2}{4\sqrt{2}G_F m_W^2}, \quad c_1^2 \equiv 1 - s_1^2, \quad (2.11)$$

see section 4.2 of [7]. Up to corrections from anomalous couplings  $s_1$  is the sine of the weak mixing angle. Two of these relations are independent of the photon or  $W$  helicities:

$$s_1^2 \mathcal{M}_{\varphi B} = c_1^2 \mathcal{M}_{\varphi W}, \quad (2.12)$$

$$s_1^2 \mathcal{M}_{\varphi \tilde{B}} = c_1^2 \mathcal{M}_{\varphi \tilde{W}}, \quad (2.13)$$

where all helicities and momenta are understood to be equal on both sides. Hence the corresponding four anomalous couplings do not appear in the amplitudes in an independent way but only as linear combinations

$$h_{\varphi WB} \equiv s_1^2 h_{\varphi W} + c_1^2 h_{\varphi B}, \quad (2.14)$$

$$h_{\varphi \tilde{W}B} \equiv s_1^2 h_{\varphi \tilde{W}} + c_1^2 h_{\varphi \tilde{B}}. \quad (2.15)$$

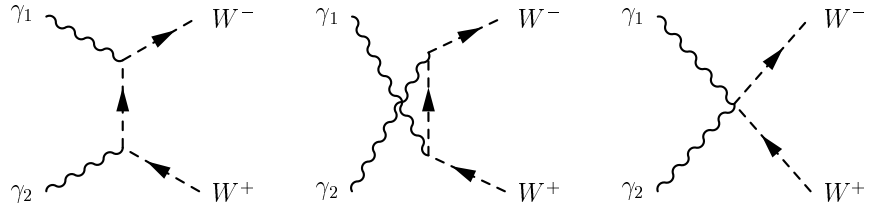


Figure 2: SM diagrams for  $\gamma\gamma \rightarrow WW$ .

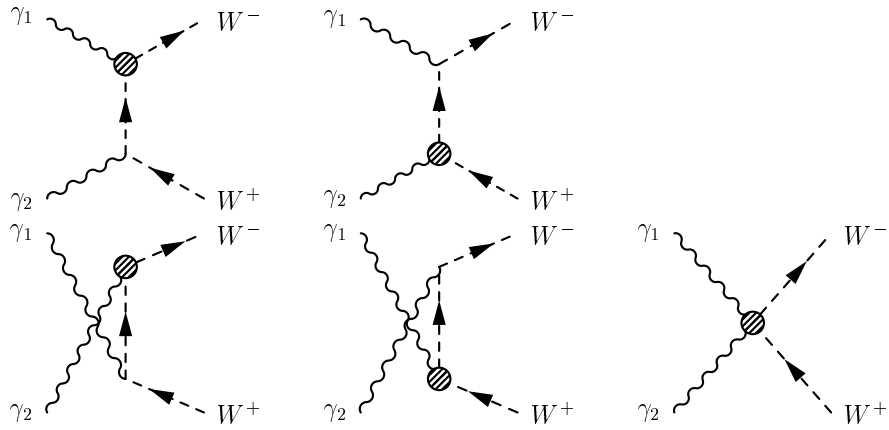


Figure 3: Diagrams with anomalous triple- or quartic-gauge-boson couplings for  $\gamma\gamma \rightarrow WW$ .

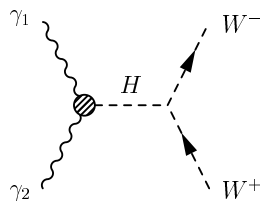


Figure 4: Diagram with anomalous  $\gamma\gamma H$  coupling for  $\gamma\gamma \rightarrow WW$ .



Another relation depends on the photon helicity  $\lambda_1$ :

$$\mathcal{M}_{\varphi\bar{W}} = 2i\lambda_1 \mathcal{M}_{\varphi W}. \quad (2.16)$$

Notice that the anomalous couplings do not modify the couplings of the  $W$  boson to fermions in the scheme  $P_W$ , see [7]. Thus there are no modifications of the decay amplitudes of the  $W$  bosons due to the  $h_i$ . We conclude that the differential cross section of  $\gamma\gamma \rightarrow WW$  is sensitive to the anomalous couplings  $h_W, h_{\bar{W}}, h_{\varphi WB}, h_{\varphi\bar{W}\bar{B}}, h_{WB}$  and  $h_{\bar{W}\bar{B}}$ . The couplings  $h_\varphi^{(1)}, h_\varphi^{(3)}$  and the orthogonal combinations to (2.14) and (2.15), that is

$$h'_{\varphi WB} = c_1^2 h_{\varphi W} - s_1^2 h_{\varphi B}, \quad (2.17)$$

$$h'_{\varphi\bar{W}\bar{B}} = c_1^2 h_{\varphi\bar{W}} - s_1^2 h_{\varphi\bar{B}}, \quad (2.18)$$

do not enter in the expressions for the amplitudes of  $\gamma\gamma \rightarrow WW$  due to (2.12) and (2.13). Thus three  $CP$  conserving couplings and one  $CP$  violating coupling are unmeasurable in  $\gamma\gamma \rightarrow WW$ .

We would like to mention some features of the differential production cross section in the SM, see Figs. 5 and 6. Its  $\cos\Theta$ -dependence can be understood from the conservation of angular momentum in the  $\gamma\gamma$  c.m. system. Photons with opposite helicities lead to an initial state with  $z$ -component of angular momentum  $\pm 2$ . From this one cannot produce  $W^-$  and  $W^+$  emitted along the  $z$  axis ( $\cos\Theta = \pm 1$ ) with identical helicities, since this would be a state with  $z$  component of angular momentum zero, see Fig. 6. However, emission at an angle  $0 < \Theta < \pi$  is possible. In the SM, two photons with identical helicities can only produce  $W$  bosons with identical helicities. Furthermore, if the photons have identical helicities and the  $W$  bosons as well, the production of  $W$  bosons with helicity different to that of the photons is suppressed with rising energy. Moreover, it is apparent from Figs. 5 and 6 that in the SM the bulk of  $W$ s is transverse and is emitted at a small angle to the beam axis, i.e.  $\cos\Theta \approx \pm 1$ .

We also want to discuss the anomalous contributions to the differential cross sections (2.5) after integration over  $\varphi, \vartheta, \bar{\varphi}, \bar{\vartheta}$ . Expanding this cross section in terms of  $h_i$ ,

$$\frac{d\sigma}{d\cos\Theta} = \frac{d\sigma_{\text{SM}}}{d\cos\Theta} + \sum_i h_i \frac{d\sigma_i}{d\cos\Theta} + O(h^2), \quad (2.19)$$

one can define the cross section contributions  $d\sigma_i/d\cos\Theta$  shown in Fig. 7 for the  $CP$ -conserving couplings. To leading order in the  $h_i$  the  $CP$ -violating contributions  $d\sigma_i/d\cos\Theta$  vanish, due to symmetry arguments, see Sect. 3. The shape of the SM and the anomalous cross section contributions varies significantly, compare Fig. 5 and Fig. 7. Thus it is possible to get some information on the  $CP$ -conserving anomalous couplings just from the differential cross section (2.19). We get information both on  $CP$ -conserving and  $CP$ -violating couplings if we take the angular distributions of the final state fermions in (2.1) into account. In the companion paper [28] this will be

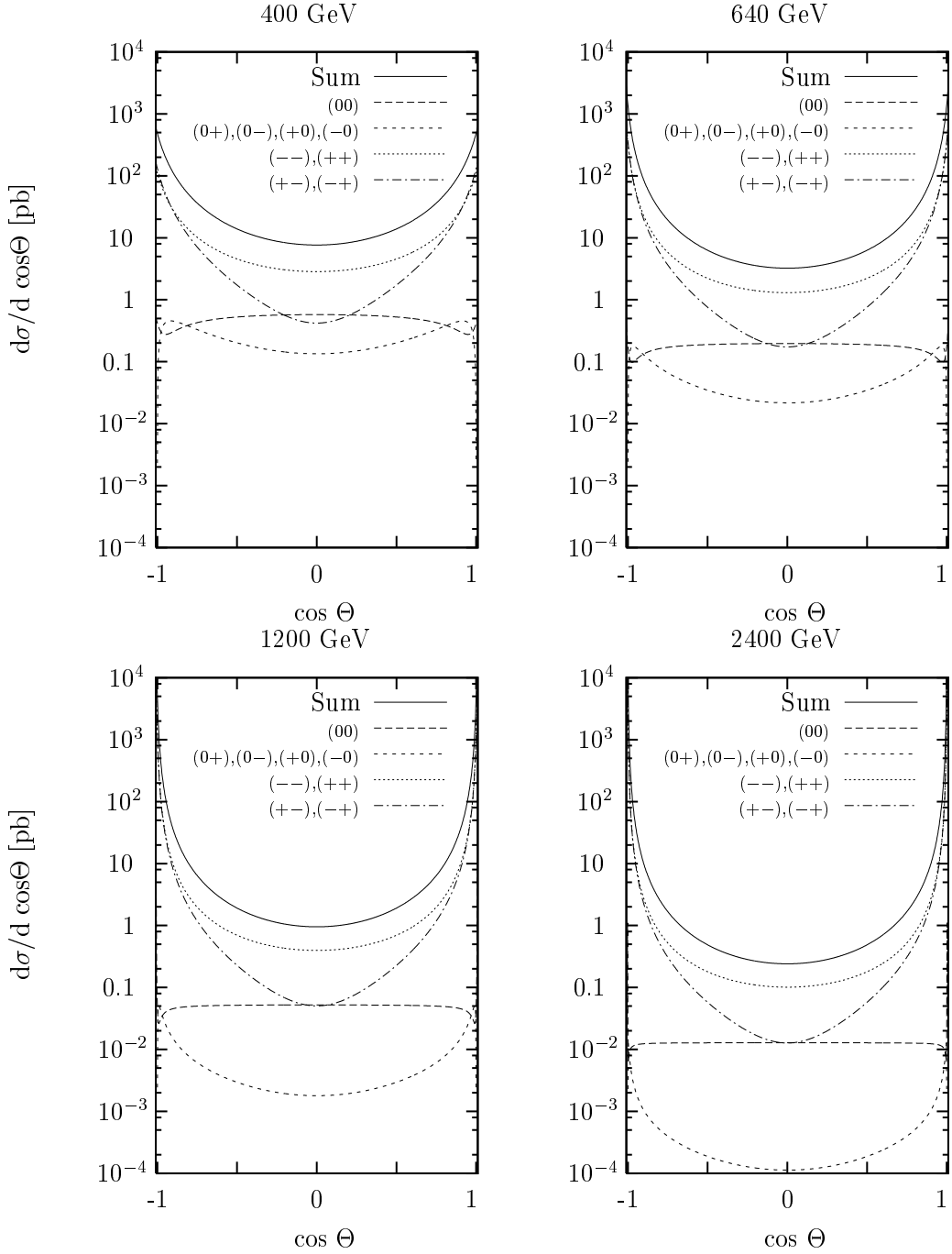


Figure 5: Differential cross section for the process  $\gamma\gamma \rightarrow WW$  in the SM with unpolarised photons at  $\gamma\gamma$  c.m. energies 400 GeV, 640 GeV, 1.2 TeV and 2.4 TeV for different helicities ( $\lambda_3, \lambda_4$ ) of the  $W$  bosons. For those curves where more than one helicity combination is indicated the curve corresponds to a single helicity combination, not to the sum.

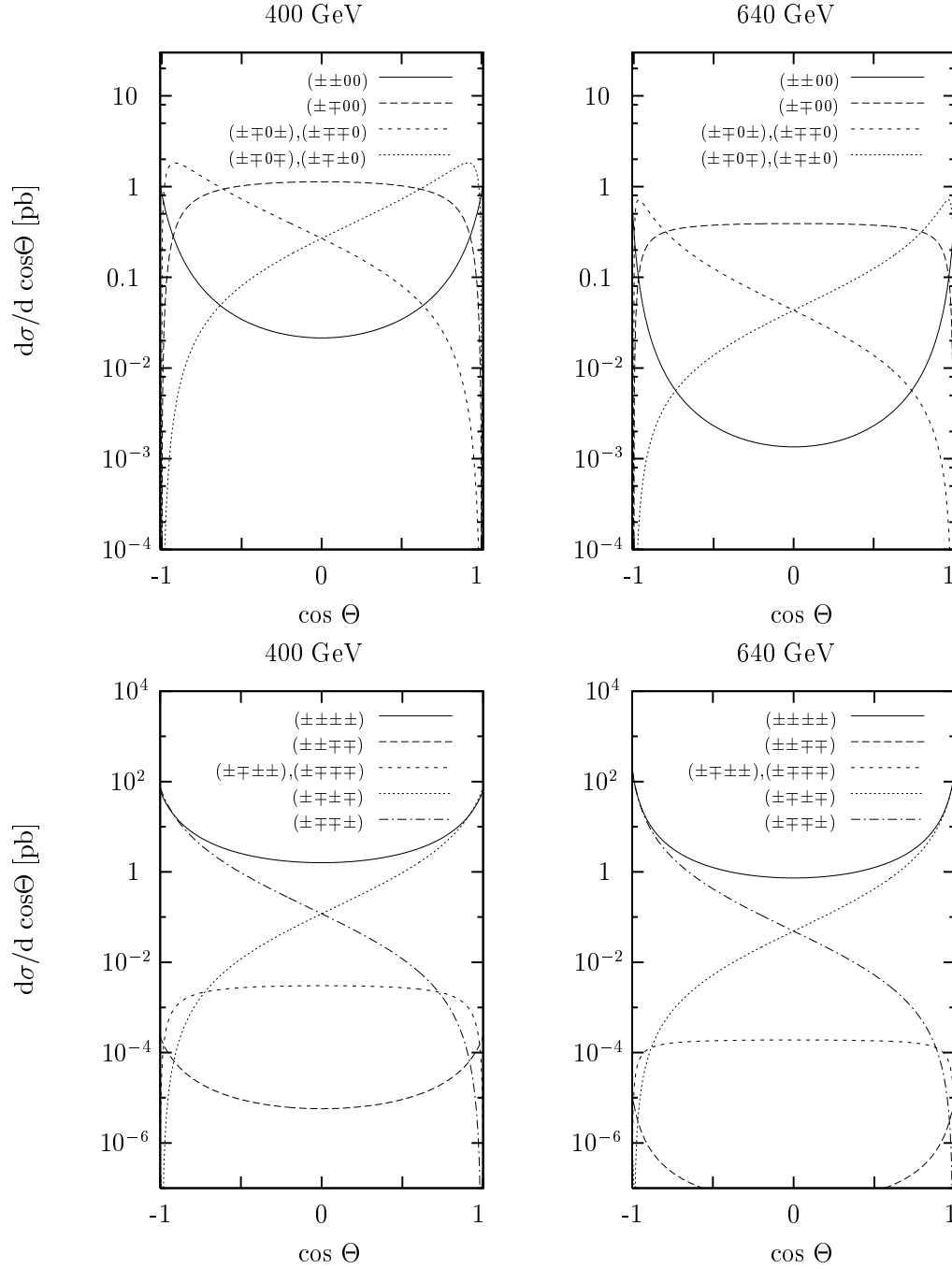


Figure 6: Differential cross section for the process  $\gamma\gamma \rightarrow WW$  in the SM for different helicities  $(\lambda_1, \lambda_2, \lambda_3, \lambda_4)$  of the photons and  $W$  bosons at  $\gamma\gamma$  c.m. energies of 400 GeV and 640 GeV. The lower part shows the cross section for purely transverse final states, whereas in the upper part one or both  $W$ s are longitudinal. For those curves where more than one helicity combination is indicated the curve corresponds to a single helicity combination, not to the sum.

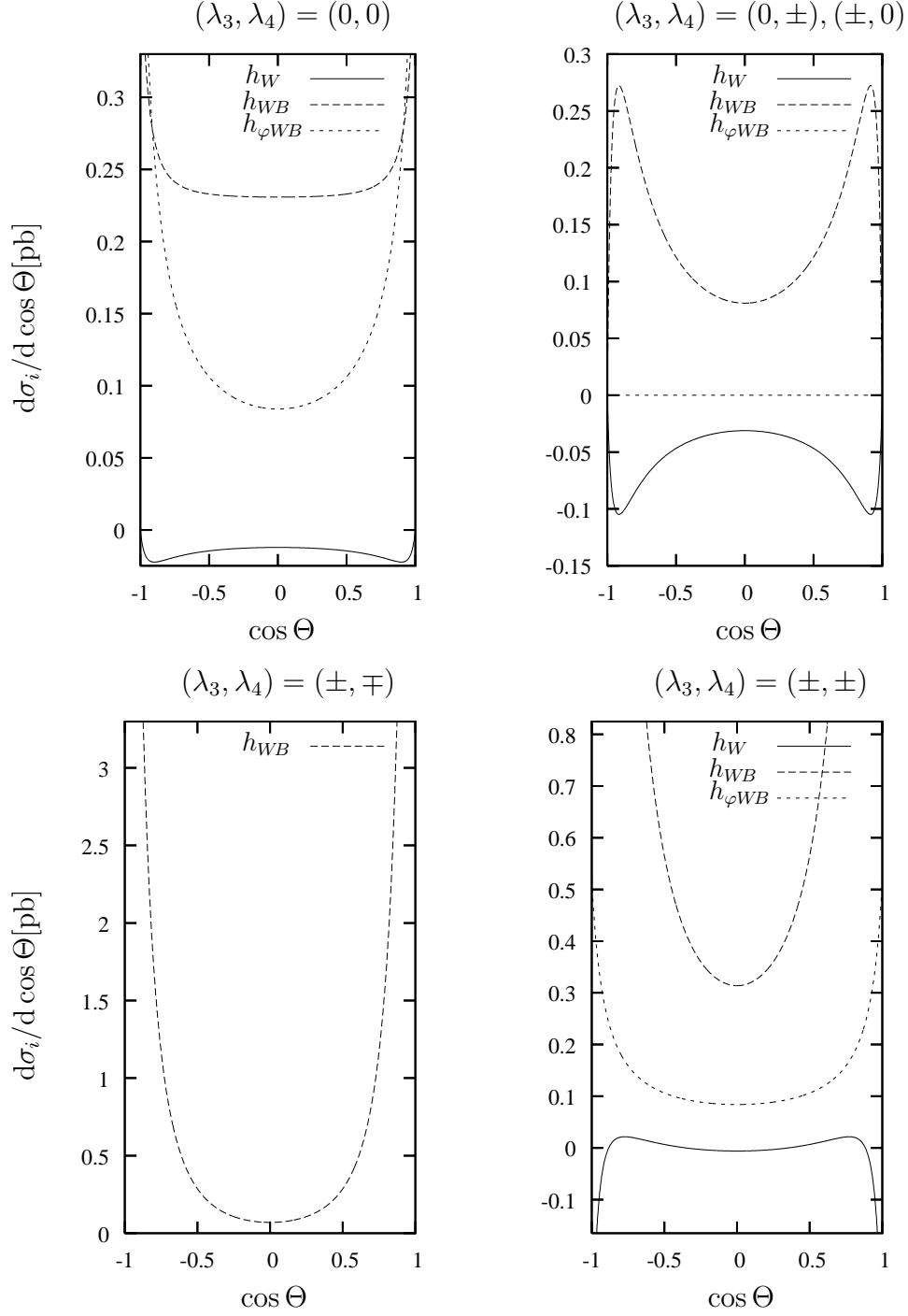


Figure 7: Anomalous contributions  $d\sigma_i/d\cos\Theta$  (2.19) to the differential cross section for the process  $\gamma\gamma \rightarrow WW$  with unpolarised photons at a  $\gamma\gamma$  c.m. energy of 400 GeV for different helicities  $(\lambda_3, \lambda_4)$  of the  $W$  bosons.

done using optimal observables which guarantee the best possible accuracy in the measurement of the anomalous couplings from a purely statistical point of view.

Finally, we discuss the total cross-section for the process  $\gamma\gamma \rightarrow WW$  for unpolarised photons including effects from anomalous couplings. In Fig. 8 we show the total SM cross section and the relative corrections  $(\sigma - \sigma_{\text{SM}})/\sigma_{\text{SM}}$  to the total cross section coming from anomalous contributions up to quadratic order in the  $h_i$ . For each of these relative corrections only one coupling  $h_i$  is different from zero. As expected, the anomalous cross sections rise with the energy if anomalous couplings are taken into account. For the three  $CP$  conserving couplings contributing to the cross section in linear order we get different contributions for positive and negative values of the couplings  $h_i$ . In the limit  $s \gg m_W^2$  only the coupling  $h_{WB}$  contributes with a linear term in  $\sigma$ , for all other couplings  $h_i$  the anomalous contributions to the total cross section are in this limit of the order  $h_i^2$ , due to the fact that the linear terms vanish after the integration over the angles related to the final fermion states. We see from Fig. 8 that for  $h_{WB} = 10^{-3}$ , the maximal value allowed from the analysis of precision observables (see table 8 of [7]), the total cross section at  $\sqrt{s} = 500$  GeV is modified only by  $\approx 0.4\%$ . The other couplings have similarly small effects already for  $h_i = 10^{-2}$ . In addition, effects in the cross section are, of course, not specific to any of the couplings. On the other hand we will show below that in the complete differential cross section (2.5) the anomalous contributions are dominated by the terms of the order  $h_i$  for reasonable energies. Typical bounds on anomalous couplings obtainable at an  $e^+e^-$  collider at  $\sqrt{s} = 500$  GeV are less than  $10^{-3}$  with optimal observables. Quadratic terms of anomalous couplings can then safely be neglected. For the total cross sections for example they would then be less than order  $10^{-4}$ .

### 3 $CP$ symmetry

To determine the sensitivity to the anomalous couplings—in particular within the framework of optimal observables considered in [28]—it is convenient to make use of the transformation properties of the amplitudes under the combined discrete symmetry  $CP$  of charge conjugation and parity reversal. Since our effective Lagrangian does not modify the SM couplings of  $W$  bosons to fermions these interactions are  $CP$  invariant as in the SM neglecting the phase in the CKM matrix. This phase plays no role in our considerations below. However the effective Lagrangian (1.2) as a whole is not  $CP$  conserving since it contains  $CP$  violating anomalous gauge-boson couplings. The primed fields of the effective Lagrangian, see App. A, transform under  $CP$  as follows:

$$A'^{\mu}(x) \rightarrow -A'_{\mu}(x'), \quad (3.1)$$

$$Z'^{\mu}(x) \rightarrow -Z'_{\mu}(x'), \quad (3.2)$$

$$W'^{\pm\mu}(x) \rightarrow -W'_{\mu}{}^{\mp}(x'), \quad (3.3)$$

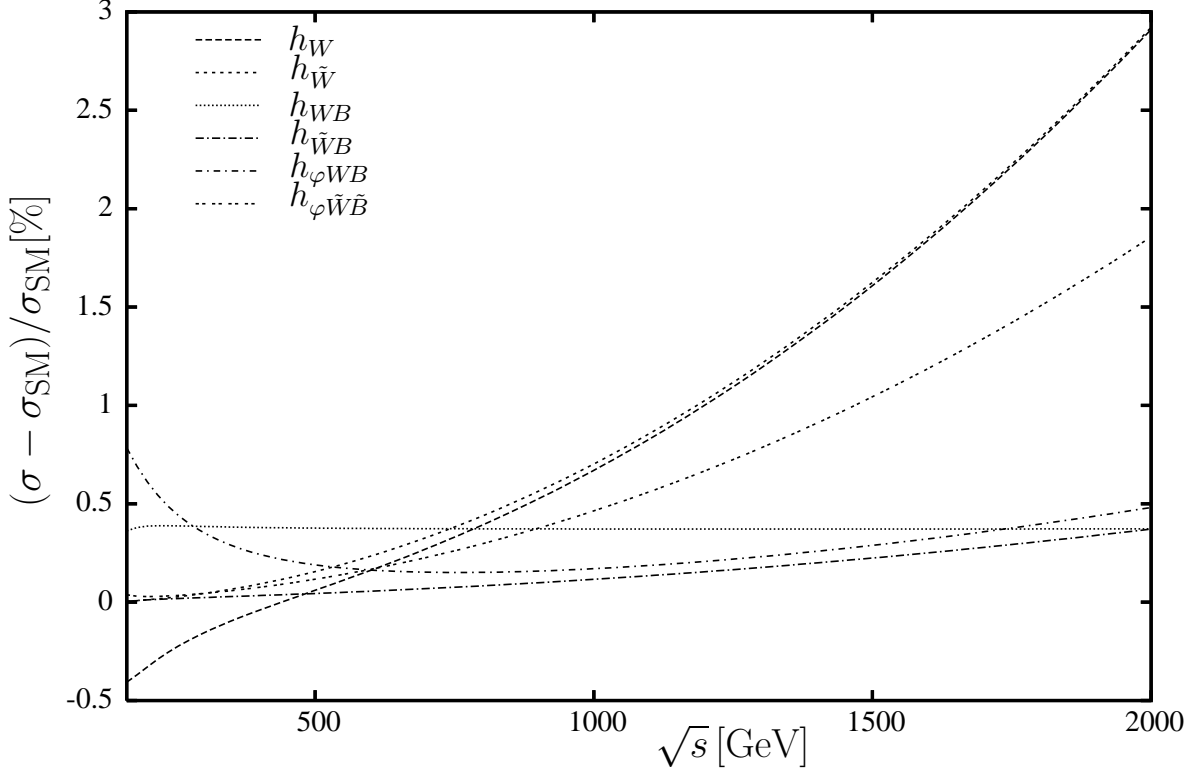


Figure 8: Total cross section for the process  $\gamma\gamma \rightarrow WW$ . We show here the unpolarised case, that is, the average over initial and sum over final-state helicities. The upper plot shows the total cross section in the SM. In the lower plot the relative corrections to the SM cross section including contributions up to quadratic order in the  $h_i$  are shown. For each of these corrections one nonvanishing coupling contribute whereas all other anomalous couplings are set to zero. The values chosen for the couplings are  $h_i = 10^{-2}$  for  $i = W, \tilde{W}, \tilde{W}B, \varphi WB, \varphi \tilde{W}\tilde{B}$  and  $h_i = 10^{-3}$  for  $i = WB$ .

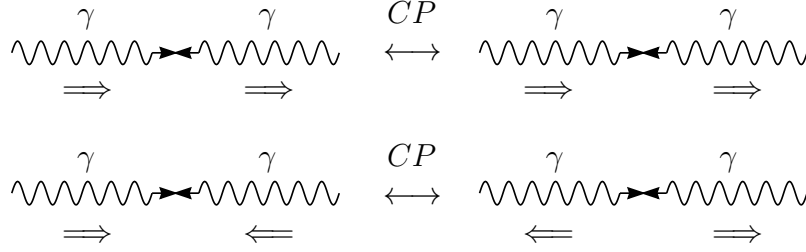


Figure 9: Behaviour of a  $\gamma\gamma$  state with opposite (top) and same (bottom) helicities under a  $CP$  transformation.

with  $x = (x^0, \mathbf{x})$  and  $x' = (x^0, -\mathbf{x})$ . Without the dimension-six operators in (1.2) the primed gauge fields are the physical fields. The Lagrangian is then the SM Lagrangian, which is invariant under the transformations (3.1) to (3.3) and an appropriate choice for the  $CP$  transformation of the other SM fields if the phase of the CKM matrix is set to zero. Considering the full Lagrangian (1.2), the physical fields, which are linear combinations of the primed fields as given in [7], transform as

$$A^\mu(x) \rightarrow -A_\mu(x'), \quad (3.4)$$

$$Z^\mu(x) \rightarrow -Z_\mu(x'), \quad (3.5)$$

$$W^{\pm\mu}(x) \rightarrow -W_\mu^\mp(x'). \quad (3.6)$$

This implies the following relations for the different parts of the amplitudes in (2.10)

$$\mathcal{M}_{\text{SM}}(\lambda_1, \lambda_2; \lambda_3, \lambda_4) = (-1)^{(\lambda_3+\lambda_4)} \mathcal{M}_{\text{SM}}(-\lambda_2, -\lambda_1; -\lambda_4, -\lambda_3), \quad (3.7)$$

$$\mathcal{M}_i(\lambda_1, \lambda_2; \lambda_3, \lambda_4) = \pi_i (-1)^{(\lambda_3+\lambda_4)} \mathcal{M}_i(-\lambda_2, -\lambda_1; -\lambda_4, -\lambda_3) \quad (3.8)$$

with  $\pi_i = +1$  for the couplings  $h_W, h_{\varphi W}, h_{\varphi B}, h_{WB}$ , and  $\pi_i = -1$  for  $h_{\tilde{W}}, h_{\varphi\tilde{W}}, h_{\varphi\tilde{B}}$  and  $h_{\tilde{W}B}$ . Particle momenta are understood to be equal on both sides of (3.7) and (3.8). From these two equations we can see that the couplings  $h_W, h_{\varphi W}, h_{\varphi B}, h_{WB}$  are  $CP$  conserving—as are  $h_\varphi^{(1)}$  and  $h_\varphi^{(3)}$ —whereas the couplings  $h_{\tilde{W}}, h_{\varphi\tilde{W}}, h_{\varphi\tilde{B}}$  and  $h_{\tilde{W}B}$  are  $CP$  violating.

Under the condition that the initial state, phase-space cuts and detector acceptance are invariant under a  $CP$  transformation, a  $CP$  odd observable gets a nonzero expectation value only if  $CP$  is violated in the interaction. Consider now the reaction  $\gamma\gamma \rightarrow WW$  for fixed photon energies in the c.m. system. The initial state is invariant under  $CP$  for unpolarised photon beams as well as for the states with  $|J_z| = 2$ , where  $J_z$  is the total angular momentum along the  $z$ -axis, see Fig. 9. For a photon collider with identical energy spectra for the two photons the same  $CP$  invariance properties hold. This will be exploited for our numerical calculations in [28] assuming unpolarised photons, so that we indeed have a  $CP$  invariant initial state. There to linear order in the  $h_i$  the expectation values of  $CP$  even (odd) optimal observables only involve the  $CP$  conserving (violating) couplings. Then—provided couplings with

the same discrete symmetry properties are grouped together—the covariance matrix of the optimal observables is block diagonal with two blocks corresponding to the  $CP$  conserving and  $CP$  violating couplings, respectively.

## 4 Conclusions

We have analysed the phenomenology of the gauge-boson sector of an electroweak effective Lagrangian that is locally  $SU(2) \times U(1)$  invariant. In addition to the SM Lagrangian we include all ten dimension-six operators that are built either only from the gauge-boson fields of the SM or from the gauge-boson fields combined with the SM-Higgs field.

We have investigated in detail the effects of the effective Lagrangian on the reaction  $\gamma\gamma \rightarrow WW$  in the photon-collider mode at an ILC. In this process the three  $CP$  conserving couplings  $h_W, h_{WB}, h_{\varphi WB}$  and the three  $CP$  violating couplings  $h_{\tilde{W}}, h_{\tilde{W}B}, h_{\varphi\tilde{W}\tilde{B}}$  are measurable, whereas the remaining three  $CP$  conserving ones  $h_{\varphi}^{(1)}, h_{\varphi}^{(3)}, h'_{\varphi WB}$  and a  $CP$  violating one  $h'_{\varphi\tilde{W}\tilde{B}}$  are not measurable, see Sect. 2. The strongest possible bounds on the anomalous couplings that can be obtained in our reaction will be computed in the companion paper [28] by means of optimal observables. There are two  $CP$  conserving and two  $CP$  violating couplings occurring both in  $\gamma\gamma \rightarrow WW$  and in  $e^+e^- \rightarrow WW$ , whereas the couplings  $h_{\varphi WB}$  and  $h_{\varphi\tilde{W}\tilde{B}}$  are only measurable in  $\gamma\gamma \rightarrow WW$ . A comparison of the sensitivity to the anomalous couplings achievable in the two reactions will be performed in [28]. Such a quantitative analysis is important to decide how much total luminosity is required in each mode of an ILC. As already explained in Sect. 1, our approach, using the effective Lagrangian (1.2) instead of form factors, is perfectly suited for a comprehensive study of all constraints on the  $h_i$  coming from different modes at an ILC and from high precision observables. We have seen that in any case the  $e^+e^-$  and the  $\gamma\gamma$  modes deliver complementary constraints on the anomalous couplings of the effective Lagrangian considered. Both modes are indispensable for a comprehensive study of the gauge-boson sector at an ILC.

## Acknowledgements

The authors are grateful to M. Diehl for reading a draft of this manuscript and to A. Denner and A. de Roeck for useful discussions. This work was supported by the German Bundesministerium für Bildung und Forschung, BMBF project no. 05HT4VHA/0, and the Deutsche Forschungsgemeinschaft through the Graduiertenkolleg “Physikalische Systeme mit vielen Freiheitsgraden”.



## A Effective Lagrangian

In this appendix we give the definition of the effective Lagrangian (1.2). For the SM Lagrangian  $\mathcal{L}_0$  we use the conventions of [31]. Restricting ourselves to the electroweak interactions and neglecting neutrino masses  $\mathcal{L}_0$  is given by

$$\begin{aligned} \mathcal{L}_0 = & -\frac{1}{4}W_{\mu\nu}^i W^{i\mu\nu} - \frac{1}{4}B_{\mu\nu} B^{\mu\nu} + (\mathcal{D}_\mu \varphi)^\dagger (\mathcal{D}^\mu \varphi) + \mu^2 \varphi^\dagger \varphi - \lambda (\varphi^\dagger \varphi)^2 \\ & + i\bar{L}\not{\mathcal{D}}L + i\bar{E}\not{\mathcal{D}}E + i\bar{Q}\not{\mathcal{D}}Q + i\bar{U}\not{\mathcal{D}}U + i\bar{D}\not{\mathcal{D}}D \\ & - (\bar{E}\Gamma_E \varphi^\dagger L + \bar{U}\Gamma_U \tilde{\varphi}^\dagger Q + \bar{D}\Gamma_D \varphi^\dagger Q + \text{H.c.}) . \end{aligned} \quad (\text{A.1})$$

The  $3 \times 3$ -Yukawa matrices have the form

$$\Gamma_E = \text{diag}(c_e, c_\mu, c_\tau), \quad (\text{A.2})$$

$$\Gamma_U = \text{diag}(c_u, c_c, c_t), \quad (\text{A.3})$$

$$\Gamma_D = V \text{diag}(c_d, c_s, c_b) V^\dagger, \quad (\text{A.4})$$

where the diagonal elements all obey  $c_i \geq 0$  and  $V$  is the CKM matrix. With these conventions the matrices  $\Gamma_E, \Gamma_U, \Gamma_D$  correspond to the matrices  $C_\ell, C'_q, C_q$  in [31], respectively. The vector of the three left-handed lepton doublets is denoted by  $L$ , of the right-handed charged leptons by  $E$ , of the left-handed quark doublets by  $Q$ , and of the right-handed up- and down-type quarks by  $U$  and  $D$ . The Higgs field is denoted by  $\varphi$ . After electroweak symmetry breaking we can choose the form

$$\varphi(x) = \frac{1}{\sqrt{2}} \begin{pmatrix} 0 \\ v + H'(x) \end{pmatrix}, \quad (\text{A.5})$$

where  $v$  is the vacuum expectation value and  $H'(x)$  is a real scalar boson field. With the full Lagrangian  $\mathcal{L}_{\text{eff}}$  (1.2) it is related to the physical Higgs-boson field  $H(x)$  through

$$H = \sqrt{1 + (h_\varphi^{(1)} + h_\varphi^{(3)})/2} H'. \quad (\text{A.6})$$

The factor depending on the anomalous couplings stems from the renormalisation of the Higgs field, see [7]. In (A.1) we have used the definitions

$$\tilde{\varphi} = \varepsilon \varphi^*, \quad \varepsilon = \begin{pmatrix} 0 & 1 \\ -1 & 0 \end{pmatrix}, \quad (\text{A.7})$$

and for the covariant derivative

$$\mathcal{D}_\mu = \partial_\mu + igW_\mu^i \mathbf{T}_i + ig' B_\mu \mathbf{Y}, \quad (\text{A.8})$$

where  $\mathbf{T}_i$  and  $\mathbf{Y}$  are the generating operators of weak-isospin and weak-hypercharge transformations. For the left-handed fermion fields and the Higgs doublet we have

	$L$	$E$	$Q$	$U$	$D$	$\varphi$
$y$	$-\frac{1}{2}$	$-1$	$\frac{1}{6}$	$\frac{2}{3}$	$-\frac{1}{3}$	$\frac{1}{2}$

Table 2: Weak hypercharges of the fermions and of the Higgs doublet.

$\mathbf{T}_i = \tau_i/2$ , where  $\tau_i$  are the Pauli matrices. For the right-handed fermion fields we have  $\mathbf{T}_i = 0$ . The hypercharges of the fermions and of the Higgs doublet are listed in Tab. 2. The field strengths are

$$W_{\mu\nu}^i = \partial_\mu W_\nu^i - \partial_\nu W_\mu^i - g \epsilon_{ijk} W_\mu^j W_\nu^k, \quad B_{\mu\nu} = \partial_\mu B_\nu - \partial_\nu B_\mu. \quad (\text{A.9})$$

Note that the signs in front of the gauge couplings in (A.8) and (A.9) differ from the conventions of [5], which leads to sign changes in some of the dimension-six operators listed below. The dimension-six operators of  $\mathcal{L}_2$  in (1.3) are defined as follows, see (3.5), (3.6), and (3.41) to (3.44) in [5],

$$O_W = \epsilon_{ijk} W_\mu^{i\nu} W_\nu^{j\lambda} W_\lambda^{k\mu}, \quad O_{\tilde{W}} = \epsilon_{ijk} \tilde{W}_\mu^{i\nu} W_\nu^{j\lambda} W_\lambda^{k\mu}, \quad (\text{A.10})$$

$$O_{\varphi W} = \frac{1}{2} (\varphi^\dagger \varphi) W_{\mu\nu}^i W^{i\mu\nu}, \quad O_{\varphi \tilde{W}} = (\varphi^\dagger \varphi) \tilde{W}_{\mu\nu}^i W^{i\mu\nu}, \quad (\text{A.11})$$

$$O_{\varphi B} = \frac{1}{2} (\varphi^\dagger \varphi) B_{\mu\nu} B^{\mu\nu}, \quad O_{\varphi \tilde{B}} = (\varphi^\dagger \varphi) \tilde{B}_{\mu\nu} B^{\mu\nu}, \quad (\text{A.12})$$

$$O_{WB} = (\varphi^\dagger \tau^i \varphi) W_{\mu\nu}^i B^{\mu\nu}, \quad O_{\tilde{W}B} = (\varphi^\dagger \tau^i \varphi) \tilde{W}_{\mu\nu}^i B^{\mu\nu}, \quad (\text{A.13})$$

$$O_\varphi^{(1)} = (\varphi^\dagger \varphi) (\mathcal{D}_\mu \varphi)^\dagger (\mathcal{D}^\mu \varphi), \quad O_\varphi^{(3)} = (\varphi^\dagger \mathcal{D}_\mu \varphi)^\dagger (\varphi^\dagger \mathcal{D}^\mu \varphi). \quad (\text{A.14})$$

The dual field strengths are

$$\tilde{W}_{\mu\nu}^i = \frac{1}{2} \epsilon_{\mu\nu\rho\sigma} W^{i\rho\sigma}, \quad \tilde{B}_{\mu\nu} = \frac{1}{2} \epsilon_{\mu\nu\rho\sigma} B^{\rho\sigma}. \quad (\text{A.15})$$

In [7] the original  $W_\mu^i$  and  $B_\mu$  fields in  $\mathcal{L}_{\text{eff}}$  are expressed in terms of the primed fields  $Z'$ ,  $A'$  and  $W'^{\pm}$  as follows:

$$W_\mu^1 = \frac{1}{\sqrt{2}} (W_\mu'^+ + W_\mu'^-), \quad W_\mu^2 = \frac{i}{\sqrt{2}} (W_\mu'^+ - W_\mu'^-), \quad (\text{A.16})$$

$$W_\mu^3 = c'_w Z'_\mu + s'_w A'_\mu, \quad B_\mu = -s'_w Z'_\mu + c'_w A'_\mu, \quad (\text{A.17})$$

where

$$s'_w \equiv \sin \theta'_w = \frac{g'}{\sqrt{g^2 + g'^2}}, \quad (\text{A.18})$$

$$c'_w \equiv \cos \theta'_w = \frac{g}{\sqrt{g^2 + g'^2}} \quad (\text{A.19})$$

are the sine and cosine of the weak mixing angle in the SM, determined by the  $SU(2)$  and  $U(1)_Y$  couplings  $g$  and  $g'$  of  $\mathcal{L}_0$ . The primed fields are the physical gauge-boson fields in absence of anomalous couplings. With anomalous couplings the  $W$ -boson field must be renormalised by a factor that depends on the  $h_i$ , similarly to the Higgs-boson field in (A.6). The physical neutral gauge-boson fields  $A$  and  $Z$  are linear combinations of  $A'$  and  $Z'$  with coefficients depending on the anomalous couplings. For these relations we refer to Sect. 3 of [7].

## B Feynman rules

In this section we list the Feynman rules that are necessary for the evaluation of the diagrams in Figs. 2 to 4 in the framework of the effective Lagrangian (1.2). These Feynman rules are obtained after expressing the field operators in (1.2) in the physical fields  $A$ ,  $Z$ ,  $W^\pm$  and  $H$ , see [7]. All constants are expressed in terms of the parameters of the  $P_W$  scheme, i.e. in terms of  $\alpha(m_Z)$ ,  $G_F$ ,  $m_W$ ,  $m_H$  and the ten anomalous couplings  $h_i$ , cf. Tab. 3 in [7]. As in [7] we use the abbreviation  $e = \sqrt{4\pi\alpha(m_Z)}$  for the positron charge at the scale of the  $Z$  mass. After linearisation in the  $h_i$  a vertex with given fields can be written as the sum of the SM vertex and the vertices proportional to the  $h_i$ . Here we list the SM vertices and the vertices proportional to the  $h_i$  separately. In all cases the momenta belonging to lines to the left of a vertex are incoming whereas those belonging to lines to the right of a vertex are outgoing. The Feynman rules for the SM vertices and for the anomalous  $\gamma WW$ ,  $\gamma\gamma WW$  and  $\gamma\gamma H$  vertices are shown in Fig. 10 and Fig. 11, respectively.

The SM vertex functions are

$$\Gamma_{\text{SM}}^{(3)\mu_1\mu_2\mu_3} = g^{\mu_1\mu_2}(q_1 + q_2)^{\mu_3} - g^{\mu_1\mu_3}(q_1 + q_3)^{\mu_2} + g^{\mu_2\mu_3}(q_3 - q_2)^{\mu_1}, \quad (\text{B.1})$$

$$\Gamma_{\text{SM}}^{(4)\mu_1\mu_2\mu_3\mu_4} = g^{\mu_1\mu_3}g^{\mu_2\mu_4} + g^{\mu_1\mu_4}g^{\mu_2\mu_3} - 2g^{\mu_1\mu_2}g^{\mu_3\mu_4}, \quad (\text{B.2})$$

$$\Gamma_{\text{SM}}^{(WWH)\mu_1\mu_2} = 2m_W^2 \left(\sqrt{2}G_F\right)^{1/2} g^{\mu_1\mu_2}. \quad (\text{B.3})$$

The figure displays three Feynman diagrams, each representing a vertex from the Standard Model Lagrangian. The diagrams are arranged vertically and each is equated to a mathematical expression.

- Top Diagram:** A wavy line representing a photon  $\gamma(q_1)$  with momentum  $\mu_1$  enters from the left. It splits into two dashed lines representing  $W^-(q_2)$  and  $W^+(q_3)$  with momenta  $\mu_2$  and  $\mu_3$  respectively, exiting to the right. This is equated to  $ie \Gamma_{\text{SM}}^{(3) \mu_1 \mu_2 \mu_3}$ .
- Middle Diagram:** Two wavy lines representing photons  $\gamma(q_1)$  and  $\gamma(q_2)$  with momenta  $\mu_1$  and  $\mu_2$  enter from the left. They meet at a central vertex and split into two dashed lines representing  $W^-(q_3)$  and  $W^+(q_4)$  with momenta  $\mu_3$  and  $\mu_4$  respectively, exiting to the right. This is equated to  $ie^2 \Gamma_{\text{SM}}^{(4) \mu_1 \mu_2 \mu_3 \mu_4}$ .
- Bottom Diagram:** A dashed line representing a Higgs boson  $H(q)$  with momentum  $\mu_1$  enters from the left. It splits into two dashed lines representing  $W^-(q_1)$  and  $W^+(q_2)$  with momenta  $\mu_1$  and  $\mu_2$  respectively, exiting to the right. This is equated to  $i \Gamma_{\text{SM}}^{(WWH) \mu_1 \mu_2}$ .

Figure 10: Feynman rules from the SM Lagrangian. The momenta of the particles are indicated in bracket. The momentum flow is always from left to right.

$$\begin{aligned}
& \mu_1 \text{---} \gamma(q_1) \text{---} \text{Vertex} \begin{cases} \nearrow W^-(q_2) \text{---} \mu_2 \\ \searrow W^+(q_3) \text{---} \mu_3 \end{cases} = ie \Gamma_{\text{an}}^{(3) \mu_1 \mu_2 \mu_3} \\
& \begin{cases} \nearrow \gamma(q_1) \text{---} \mu_1 \\ \searrow \gamma(q_2) \text{---} \mu_2 \end{cases} \text{---} \text{Vertex} \begin{cases} \nearrow W^-(q_3) \text{---} \mu_3 \\ \searrow W^+(q_4) \text{---} \mu_4 \end{cases} = ie^2 \Gamma_{\text{an}}^{(4) \mu_1 \mu_2 \mu_3 \mu_4} \\
& \begin{cases} \nearrow \gamma(q_1) \text{---} \mu_1 \\ \searrow \gamma(q_2) \text{---} \mu_2 \end{cases} \text{---} \text{Vertex} \text{---} H(q) = i \Gamma_{\text{an}}^{(\gamma\gamma H) \mu_1 \mu_2}
\end{aligned}$$

Figure 11: Feynman rules for the anomalous vertices. The momenta of the particles are indicated in brackets. The momentum flow is always from left to right.

The anomalous vertex functions are (for the definition of  $s_1$  and  $c_1$  see Eq. (2.11)):

$$\begin{aligned}
\Gamma_{\text{an}}^{(3)\mu_1\mu_2\mu_3} &= 6h_W \sqrt{2}G_F \frac{s_1}{e} \left( q_2^{\mu_1} q_3^{\mu_2} q_1^{\mu_3} - q_3^{\mu_1} q_1^{\mu_2} q_2^{\mu_3} \right. \\
&\quad + (g^{\mu_2\mu_3} q_3^{\mu_1} - g^{\mu_1\mu_3} q_3^{\mu_2}) q_1 \cdot q_2 \\
&\quad + (g^{\mu_1\mu_2} q_2^{\mu_3} - g^{\mu_2\mu_3} q_2^{\mu_1}) q_1 \cdot q_3 \\
&\quad \left. + (g^{\mu_1\mu_3} q_1^{\mu_2} - g^{\mu_1\mu_2} q_1^{\mu_3}) q_2 \cdot q_3 \right) \\
&\quad + 6h_{\tilde{W}} \sqrt{2}G_F \frac{s_1}{e} \left( q_3^{\mu_2} \epsilon^{\mu_1\mu_3\rho\sigma} q_{1\rho} q_{2\sigma} - q_2^{\mu_3} \epsilon^{\mu_1\mu_2\rho\sigma} q_{1\rho} q_{3\sigma} \right. \\
&\quad \left. - g^{\mu_2\mu_3} \epsilon^{\mu_1\nu\rho\sigma} q_{1\nu} q_{2\rho} q_{3\sigma} - q_2 \cdot q_3 \epsilon^{\mu_1\mu_2\mu_3\sigma} q_{1\sigma} \right) \\
&\quad + h_{WB} \frac{c_1}{s_1} (g^{\mu_1\mu_2} q_1^{\mu_3} - g^{\mu_1\mu_3} q_1^{\mu_2}) \\
&\quad + h_{\tilde{W}B} \frac{c_1}{s_1} \epsilon^{\mu_1\mu_2\mu_3\sigma} q_{1\sigma},
\end{aligned} \tag{B.4}$$

$$\begin{aligned}
\Gamma_{\text{an}}^{(4)\mu_1\mu_2\mu_3\mu_4} &= -6h_W \sqrt{2}G_F \frac{s_1}{e} \left( g^{\mu_1\mu_2} g^{\mu_3\mu_4} (q_1 + q_2) \cdot (q_3 + q_4) \right. \\
&\quad - g^{\mu_2\mu_3} g^{\mu_1\mu_4} (q_2 \cdot q_4 + q_1 \cdot q_3) \\
&\quad - g^{\mu_1\mu_3} g^{\mu_2\mu_4} (q_1 \cdot q_4 + q_2 \cdot q_3) \\
&\quad + g^{\mu_1\mu_3} \left( q_1^{\mu_4} (q_4 - q_3)^{\mu_2} + q_2^{\mu_4} q_3^{\mu_2} + q_1^{\mu_2} q_3^{\mu_4} \right) \\
&\quad + g^{\mu_1\mu_4} \left( q_1^{\mu_3} (q_3 - q_4)^{\mu_2} + q_2^{\mu_3} q_4^{\mu_2} + q_1^{\mu_2} q_4^{\mu_3} \right) \\
&\quad + g^{\mu_2\mu_3} \left( q_2^{\mu_4} (q_4 - q_3)^{\mu_1} + q_1^{\mu_4} q_3^{\mu_1} + q_2^{\mu_1} q_3^{\mu_4} \right) \\
&\quad + g^{\mu_2\mu_4} \left( q_2^{\mu_3} (q_3 - q_4)^{\mu_1} + q_1^{\mu_3} q_4^{\mu_1} + q_2^{\mu_1} q_4^{\mu_3} \right) \\
&\quad - g^{\mu_1\mu_2} \left( (q_1 + q_2)^{\mu_3} q_3^{\mu_4} + (q_1 + q_2)^{\mu_4} q_4^{\mu_3} \right) \\
&\quad \left. - g^{\mu_3\mu_4} \left( (q_3 + q_4)^{\mu_2} q_2^{\mu_1} + (q_3 + q_4)^{\mu_1} q_1^{\mu_2} \right) \right) \\
&\quad - 6h_{\tilde{W}} \sqrt{2}G_F \frac{s_1}{e} \left( g^{\mu_1\mu_3} \epsilon^{\mu_2\mu_4\rho\sigma} q_{2\rho} q_{3\sigma} + g^{\mu_1\mu_4} \epsilon^{\mu_2\mu_3\rho\sigma} q_{2\rho} q_{4\sigma} \right. \\
&\quad + (q_4 - q_3)^{\mu_1} \epsilon^{\mu_2\mu_3\mu_4\sigma} q_{2\sigma} + g^{\mu_2\mu_3} \epsilon^{\mu_1\mu_4\rho\sigma} q_{1\rho} q_{3\sigma} \\
&\quad + (q_4 - q_3)^{\mu_2} \epsilon^{\mu_1\mu_3\mu_4\sigma} q_{1\sigma} + g^{\mu_2\mu_4} \epsilon^{\mu_1\mu_3\rho\sigma} q_{1\rho} q_{4\sigma} \\
&\quad + g^{\mu_3\mu_4} \epsilon^{\mu_1\mu_2\rho\sigma} (q_2 - q_1)_\rho (q_3 + q_4)_\sigma \\
&\quad \left. + q_4^{\mu_3} \epsilon^{\mu_1\mu_2\mu_4\sigma} (q_2 - q_1)_\sigma + q_3^{\mu_4} \epsilon^{\mu_1\mu_2\mu_3\sigma} (q_2 - q_1)_\sigma \right),
\end{aligned} \tag{B.5}$$

$$\begin{aligned}
\Gamma_{\text{an}}^{(\gamma\gamma H)\mu_1\mu_2} &= 2(h_{\varphi WB} - 2h_{WB}s_1c_1) (q_1^{\mu_2} q_2^{\mu_1} - g^{\mu_1\mu_2} q_1 \cdot q_2) \\
&\quad + 4(h_{\varphi\tilde{W}B} - h_{\tilde{W}B}s_1c_1) \epsilon^{\mu_1\mu_2\rho\sigma} q_{1\rho} q_{2\sigma}.
\end{aligned} \tag{B.6}$$

Here the centred dots denote invariant four products. The Feynman rules for the

$W$ -boson decays in the  $P_W$  scheme are identical to the SM ones.

## C Particle momenta and polarisations

The production process  $\gamma\gamma \rightarrow WW$  is calculated in the c.m. system of the two photons. Our coordinates are defined in Sect. 2. For the incoming photons and outgoing  $W$  bosons we use the polarisation vectors

$$\epsilon_1^\mu(\lambda_1) = \frac{1}{\sqrt{2}}(0, -\lambda_1, -i, 0), \quad (\text{C.1})$$

$$\epsilon_2^\mu(\lambda_2) = \frac{1}{\sqrt{2}}(0, \lambda_2, -i, 0), \quad (\text{C.2})$$

$$\epsilon_3^\mu(\lambda_3)^* = \frac{1}{\sqrt{2}}(0, -\lambda_3 \cos \Theta, i, \lambda_3 \sin \Theta), \quad (\text{C.3})$$

$$\epsilon_4^\mu(\lambda_4)^* = \frac{1}{\sqrt{2}}(0, \lambda_4 \cos \Theta, i, -\lambda_4 \sin \Theta), \quad (\text{C.4})$$

$$\epsilon_3^\mu(0)^* = \frac{\sqrt{s}}{2m_W}(\beta, \sin \Theta, 0, \cos \Theta), \quad (\text{C.5})$$

$$\epsilon_4^\mu(0)^* = \frac{\sqrt{s}}{2m_W}(\beta, -\sin \Theta, 0, -\cos \Theta), \quad (\text{C.6})$$

where  $\beta = (1 - 4m_W^2/s)^{1/2}$  and the asterisk denotes complex conjugation. The helicities  $\lambda_1$  and  $\lambda_2$  of the photons and  $\lambda_3$  and  $\lambda_4$  of the  $W$  bosons take *only* the values  $+1$  or  $-1$  here. The vectors of longitudinal polarisation of the  $W$ s are separately given in the last two equations. In the frames specified in Sect. 2 (see (2.5) and the following equations), the four-momenta of the final-state fermions are

$$p_1^\mu = \frac{1}{2}\sqrt{k_3^2} (1, \sin \vartheta \cos \varphi, \sin \vartheta \sin \varphi, \cos \vartheta), \quad (\text{C.7})$$

$$p_2^\mu = \frac{1}{2}\sqrt{k_3^2} (1, -\sin \vartheta \cos \varphi, -\sin \vartheta \sin \varphi, -\cos \vartheta), \quad (\text{C.8})$$

$$p_3^\mu = \frac{1}{2}\sqrt{k_4^2} (1, -\sin \bar{\vartheta} \cos \bar{\varphi}, -\sin \bar{\vartheta} \sin \bar{\varphi}, -\cos \bar{\vartheta}), \quad (\text{C.9})$$

$$p_4^\mu = \frac{1}{2}\sqrt{k_4^2} (1, \sin \bar{\vartheta} \cos \bar{\varphi}, \sin \bar{\vartheta} \sin \bar{\varphi}, \cos \bar{\vartheta}). \quad (\text{C.10})$$

Here we neglected all masses of the final state fermions.

## D Helicity amplitudes

In this section we list the helicity amplitudes for  $\gamma\gamma \rightarrow WW$  in (2.6) and the relevant  $l$ -functions describing the  $W$ -decay amplitudes in (2.8) and (2.9).

In the helicity amplitudes  $\mathcal{M}(\lambda_1, \lambda_2; \lambda_3, \lambda_4)$  in (2.6) altogether 36 combinations of the photon helicities  $\lambda_1$  and  $\lambda_2$  and  $W$ -boson helicities  $\lambda_3$  and  $\lambda_4$  are possible. In order to give the amplitudes in a convenient way we distinguish between longitudinal and transverse  $W$  helicities. Thus, in the following

$$\lambda_1, \lambda_2, \lambda_3, \lambda_4 = \pm 1, \quad (\text{D.1})$$

whereas the amplitudes where one or both  $W$  bosons have longitudinal polarisation are listed separately. The amplitudes  $\mathcal{M}(\lambda_1, \lambda_2; 0, \lambda_4)$  can be obtained from the amplitudes  $\mathcal{M}(\lambda_1, \lambda_2; \lambda_3, 0)$  by the replacements ( $\lambda_3 \rightarrow \lambda_4$ ) and ( $\lambda_1 \leftrightarrow \lambda_2$ ). We use the abbreviations

$$A = (1 - \beta^2 \cos^2 \Theta), \quad B = s - m_H^2, \quad (\text{D.2})$$

$$\beta = \sqrt{1 - 4m_W^2/s}, \quad \gamma = \frac{1}{\sqrt{1 - \beta^2}} = \frac{\sqrt{s}}{2m_W}. \quad (\text{D.3})$$

For the SM amplitudes we obtain

$$\mathcal{M}_{\text{SM}}(\lambda_1, \lambda_2; 0, 0) = \frac{ie^2}{\gamma^2 A} ((\gamma^2 + 1)(1 - \lambda_1 \lambda_2) \sin^2 \Theta - (1 + \lambda_1 \lambda_2)), \quad (\text{D.4})$$

$$\mathcal{M}_{\text{SM}}(\lambda_1, \lambda_2; \lambda_3, 0) = \frac{-ie^2 \sqrt{2}}{\gamma A} (\lambda_1 - \lambda_2)(1 + \lambda_1 \lambda_3 \cos \Theta) \sin \Theta, \quad (\text{D.5})$$

$$\begin{aligned} \mathcal{M}_{\text{SM}}(\lambda_1, \lambda_2; \lambda_3, \lambda_4) = \frac{-ie^2}{2A} & \left( 2\beta(\lambda_1 + \lambda_2)(\lambda_3 + \lambda_4) \right. \\ & - \gamma^{-2}(1 + \lambda_3 \lambda_4)(2\lambda_1 \lambda_2 + (1 - \lambda_1 \lambda_2) \cos^2 \Theta) \\ & + (1 + \lambda_1 \lambda_2 \lambda_3 \lambda_4)(3 + \lambda_1 \lambda_2) \\ & + 2(\lambda_1 - \lambda_2)(\lambda_3 - \lambda_4) \cos \Theta \\ & \left. + (1 - \lambda_1 \lambda_2)(1 - \lambda_3 \lambda_4) \cos^2 \Theta \right). \end{aligned} \quad (\text{D.6})$$

These results agree with [22] apart from an overall factor of  $-i$ . Note their different definition of  $\gamma$  (they use  $\gamma = s/m_W^2$ ).



The following results are obtained for the parts of the amplitudes (2.10) that multiply an anomalous coupling where the subscript denotes the corresponding coupling, see (2.11) for the coefficients  $s_1$  and  $c_1$ :

$$\mathcal{M}_W(\lambda_1, \lambda_2; 0, 0) = \frac{3iess_1\sqrt{2}G_F}{\gamma^2 A} \sin^2 \Theta (1 + \lambda_1 \lambda_2), \quad (\text{D.7})$$

$$\begin{aligned} \mathcal{M}_W(\lambda_1, \lambda_2; \lambda_3, 0) &= \frac{3iess_1 G_F}{2\gamma A} \sin \Theta \\ &\times \left( (\lambda_1 - \lambda_2)\beta^2 - \beta \cos \Theta (\lambda_1 + \lambda_2) - 2\lambda_3 \cos \Theta (\lambda_1 \lambda_2 + \gamma^{-2}) \right), \end{aligned} \quad (\text{D.8})$$

$$\begin{aligned} \mathcal{M}_W(\lambda_1, \lambda_2; \lambda_3, \lambda_4) &= \frac{3iess_1\sqrt{2}G_F}{4A} \left( -\gamma^{-2}\beta(1 + \cos^2 \Theta)(\lambda_1 + \lambda_2)(\lambda_3 + \lambda_4) \right. \\ &+ 2\sin^2 \Theta (3 + \lambda_3\lambda_4 + \lambda_1\lambda_2(1 - \lambda_3\lambda_4) - \beta(\lambda_1 + \lambda_2)(\lambda_3 + \lambda_4)) \\ &\left. - 2\gamma^{-2}(2 + (1 - \lambda_1\lambda_2)\lambda_3\lambda_4 - \cos^2 \Theta(3 + \lambda_1\lambda_2 + 2\lambda_3\lambda_4)) \right), \end{aligned} \quad (\text{D.9})$$

$$\mathcal{M}_{\tilde{W}}(\lambda_1, \lambda_2; 0, 0) = -\frac{3ess_1\sqrt{2}G_F}{\gamma^2 A} \sin^2 \Theta (\lambda_1 + \lambda_2), \quad (\text{D.10})$$

$$\begin{aligned} \mathcal{M}_{\tilde{W}}(\lambda_1, \lambda_2; \lambda_3, 0) &= \frac{3ess_1 G_F}{2\gamma A} \sin \Theta \\ &\times \left( \beta(\lambda_1 - \lambda_2)\lambda_3 + \cos \Theta (2\beta + (2 - \beta^2)(\lambda_1 + \lambda_2)\lambda_3) \right), \end{aligned} \quad (\text{D.11})$$

$$\begin{aligned} \mathcal{M}_{\tilde{W}}(\lambda_1, \lambda_2; \lambda_3, \lambda_4) &= -\frac{3ess_1 G_F}{\sqrt{2}A} \left( 2\sin^2 \Theta (\lambda_1 + \lambda_2 - \beta(\lambda_3 + \lambda_4)) \right. \\ &+ \gamma^{-2} \left( (\lambda_1 + \lambda_2)(\cos^2 \Theta(2 + \lambda_3\lambda_4) - 1) \right. \\ &\left. \left. - \beta(\cos^2 \Theta + \lambda_1\lambda_2)(\lambda_3 + \lambda_4) \right) \right), \end{aligned} \quad (\text{D.12})$$

$$\mathcal{M}_{\varphi W}(\lambda_1, \lambda_2; 0, 0) = -\frac{is^2 s_1^2 \sqrt{2}G_F}{4B} (1 + \beta^2)(1 + \lambda_1 \lambda_2), \quad (\text{D.13})$$

$$\mathcal{M}_{\varphi W}(\lambda_1, \lambda_2; \lambda_3, 0) = 0, \quad (\text{D.14})$$

$$\mathcal{M}_{\varphi W}(\lambda_1, \lambda_2; \lambda_3, \lambda_4) = -\frac{is^2 s_1^2 \sqrt{2}G_F}{8\gamma^2 B} (1 + \lambda_1 \lambda_2)(1 + \lambda_3 \lambda_4), \quad (\text{D.15})$$

$$\mathcal{M}_{\varphi\bar{W}} = 2i\lambda_1 \mathcal{M}_{\varphi W}, \quad (\text{D.16})$$

$$\mathcal{M}_{\varphi B} = \frac{c_1^2}{s_1^2} \mathcal{M}_{\varphi W}, \quad (\text{D.17})$$

$$\mathcal{M}_{\varphi\bar{B}} = \frac{c_1^2}{s_1^2} \mathcal{M}_{\varphi\bar{W}}, \quad (\text{D.18})$$

$$\begin{aligned} \mathcal{M}_{WB}(\lambda_1, \lambda_2; 0, 0) &= \frac{2ie^2 c_1}{A s_1} (1 - \lambda_1 \lambda_2 - 2 \cos^2 \Theta - \gamma^2 (1 + \lambda_1 \lambda_2) \sin^2 \Theta) \\ &\quad + \frac{is^2 G_F}{\sqrt{2}B} s_1 c_1 (1 + \beta^2) (1 + \lambda_1 \lambda_2), \end{aligned} \quad (\text{D.19})$$

$$\begin{aligned} \mathcal{M}_{WB}(\lambda_1, \lambda_2; \lambda_3, 0) &= \frac{ie^2 \gamma c_1}{\sqrt{2}A s_1} \sin \Theta \left( (\lambda_2 - \lambda_1) (1 + \gamma^{-2}) \right. \\ &\quad \left. + (\beta(\lambda_1 + \lambda_2) + 2\lambda_3(\lambda_1 \lambda_2 - \gamma^{-2})) \cos \Theta \right), \end{aligned} \quad (\text{D.20})$$

$$\begin{aligned} \mathcal{M}_{WB}(\lambda_1, \lambda_2; \lambda_3, \lambda_4) &= -\frac{ie^2 c_1}{2A s_1} \left( \beta(\lambda_1 + \lambda_2)(\lambda_3 + \lambda_4)(1 + \cos^2 \Theta) \right. \\ &\quad \left. + 2 \left( 2 + (\lambda_1 - \lambda_2)(\lambda_3 - \lambda_4) \cos \Theta \right. \right. \\ &\quad \left. \left. + ((\lambda_1 \lambda_2 - 1) \cos^2 \Theta + 1 + \lambda_1 \lambda_2) \lambda_3 \lambda_4 \right) \right) \\ &\quad + \frac{is^2 \sqrt{2} G_F}{4\gamma^2 B} s_1 c_1 (1 + \lambda_1 \lambda_2) (1 + \lambda_3 \lambda_4), \end{aligned} \quad (\text{D.21})$$

$$\mathcal{M}_{\bar{W}B}(\lambda_1, \lambda_2; 0, 0) = 2e^2 \frac{c_1}{s_1} \gamma^2 (\lambda_1 + \lambda_2) - \frac{s^2 G_F}{\sqrt{2}B} s_1 c_1 (1 + \beta^2) (\lambda_1 + \lambda_2), \quad (\text{D.22})$$

$$\begin{aligned} \mathcal{M}_{\bar{W}B}(\lambda_1, \lambda_2; \lambda_3, 0) &= \frac{e^2 \gamma c_1}{\sqrt{2}A s_1} \sin \Theta \\ &\quad \times \left( \beta(\lambda_2 - \lambda_1) \lambda_3 - \cos \Theta (2\beta + \beta^2(\lambda_1 + \lambda_2) \lambda_3) \right), \end{aligned} \quad (\text{D.23})$$

$$\begin{aligned} \mathcal{M}_{\bar{W}B}(\lambda_1, \lambda_2; \lambda_3, \lambda_4) &= \frac{e^2 c_1^2}{A s_1} (\lambda_3(\lambda_1 + \lambda_2) + \beta(\lambda_1 \lambda_2 + \cos^2 \Theta)) (\lambda_3 + \lambda_4) \\ &\quad - \frac{s^2 \sqrt{2} G_F}{4\gamma^2 B} s_1 c_1^2 (\lambda_1 + \lambda_2) (1 + \lambda_3 \lambda_4). \end{aligned} \quad (\text{D.24})$$

The  $l$ -functions used in (2.8) and (2.9) are given by

$$l_- = d_+(\vartheta)e^{-i\varphi}, \quad l_0 = -d_0(\vartheta), \quad l_+ = d_-(\vartheta)e^{i\varphi}, \quad (\text{D.25})$$

$$\bar{l}_- = d_+(\bar{\vartheta})e^{i\bar{\varphi}}, \quad \bar{l}_0 = -d_0(\bar{\vartheta}), \quad \bar{l}_+ = d_-(\bar{\vartheta})e^{-i\bar{\varphi}} \quad (\text{D.26})$$

with  $d_{\pm}(x) = (1 \pm \cos x)/\sqrt{2}$  and  $d_0(x) = \sin x$ .

## References

- [1] “TESLA Technical Design Report Part I: Executive Summary,” eds. F. Richard, J. R. Schneider, D. Trines and A. Wagner, DESY, Hamburg, 2001 [hep-ph/0106314];  
“TESLA Technical Design Report Part III: Physics at an  $e^+e^-$  Linear Collider,” eds. R.-D. Heuer, D. Miller, F. Richard, P. M. Zerwas, DESY, Hamburg, 2001 [hep-ph/0106315].
- [2] J. R. Ellis, E. Keil and G. Rolandi, “Options for Future Colliders at CERN,” CERN-EP-98-03;  
J. P. Delahaye *et al.*, “CLIC—a Two-Beam Multi-TeV  $e^+e^-$  Linear Collider,” in: *Proc. of the 20th Intl. Linac Conference LINAC 2000* ed. Alexander W. Chao, eConf C000821, MO201 (2000) [physics/0008064];  
E. Accomando *et al.* [CLIC Physics Working Group Collaboration], “Physics at the CLIC multi-TeV linear collider,” CERN, Geneva, 2004, [arXiv:hep-ph/0412251].
- [3] “TESLA Technical Design Report, Part VI, Chapter 1: Photon Collider at TESLA,” B. Badelek *et al.*, DESY, Hamburg, 2001, [hep-ex/0108012].
- [4] H. Burkhardt and V. Telnov, “CLIC 3-TeV Photon Collider Option,” CERN-SL-2002-013-AP.
- [5] W. Buchmüller and D. Wyler, Nucl. Phys. B **268**, 621 (1986).
- [6] C. N. Leung, S. T. Love and S. Rao, Z. Phys. C **31**, 433 (1986).
- [7] O. Nachtmann, F. Nagel and M. Pospischil, Eur. Phys. J. C **42** (2005) 139 [arXiv:hep-ph/0404006].
- [8] K. Hagiwara, S. Ishihara, R. Szalapski and D. Zeppenfeld, Phys. Lett. B **283**, 353 (1992);  
K. Hagiwara, S. Ishihara, R. Szalapski and D. Zeppenfeld, Phys. Rev. D **48**, 2182 (1993).
- [9] K. Hagiwara, R. D. Peccei, D. Zeppenfeld and K. Hikasa, Nucl. Phys. B **282**, 253 (1987).

- [10] M. Diehl, O. Nachtmann and F. Nagel, Eur. Phys. J. C **27**, 375 (2003) [hep-ph/0209229];  
M. Diehl, O. Nachtmann and F. Nagel, Eur. Phys. J. C **32**, 17 (2003) [hep-ph/0306247].
- [11] M. Diehl and O. Nachtmann, Z. Phys. C **62**, 397 (1994);  
M. Diehl and O. Nachtmann, Eur. Phys. J. C **1**, 177 (1998) [hep-ph/9702208].
- [12] K. J. F. Gaemers and G. J. Gounaris, Z. Phys. C **1**, 259 (1979).
- [13] F. A. Berends *et al.*, “Report of the working group on the measurement of triple gauge boson couplings,” J. Phys. G **24**, 405 (1998) [hep-ph/9709413].
- [14] W. Menges, “A study of charged current triple gauge couplings at TESLA,” LC-PHSM-2001-022.
- [15] T. Abe *et al.* [American Linear Collider Working Group Collaboration], in *Proc. of the APS/DPF/DPB Summer Study on the Future of Particle Physics (Snowmass 2001)* ed. N. Graf, SLAC-R-570 *Resource book for Snowmass 2001, 30 Jun - 21 Jul 2001, Snowmass, Colorado*.
- [16] I. Kuss and E. Nuss, Eur. Phys. J. C **4**, 641 (1998) [hep-ph/9706406].
- [17] I. Božović-Jelisavčić, K. Mönig and J. Šekarić, “Measurement of trilinear gauge couplings at a  $\gamma\gamma$  and  $e\gamma$  collider,” hep-ph/0210308;  
K. Mönig, “Electroweak Gauge Theories and Alternative Theories at a Future Linear  $e^+e^-$  Collider,” hep-ph/0309021.
- [18] G. Tupper and M. A. Samuel, Phys. Rev. D **23** (1981) 1933;  
S. Y. Choi and F. Schrempp, Phys. Lett. B **272** (1991) 149;  
E. Yehudai, Phys. Rev. D **44** (1991) 3434.
- [19] G. Bélanger and F. Boudjema, Phys. Lett. B **288** (1992) 210.
- [20] I. B. Marfin, V. A. Mossolov and T. V. Shishkina, “Anomalous quartic boson couplings via  $\gamma\gamma \rightarrow W^+W^-$  and  $\gamma\gamma \rightarrow W^+W^-Z$  at the TESLA kinematics,” hep-ph/0304250.
- [21] G. Bélanger and G. Couture, Phys. Rev. D **49** (1994) 5720.
- [22] M. Baillargeon, G. Bélanger and F. Boudjema, Nucl. Phys. B **500** (1997) 224 [hep-ph/9701372].
- [23] A. Bredenstein, S. Dittmaier and M. Roth, Eur. Phys. J. C **36** (2004) 341 [hep-ph/0405169].

- [24] A. Bredenstein, S. Dittmaier and M. Roth, *Eur. Phys. J. C* **44** (2005) 27 [hep-ph/0506005].
- [25] A. T. Banin, I. F. Ginzburg and I. P. Ivanov, *Phys. Rev. D* **59** (1999) 115001 [arXiv:hep-ph/9806515];  
E. Gabrielli, V. A. Ilyin and B. Mele, *Phys. Rev. D* **60** (1999) 113005 [arXiv:hep-ph/9902362].
- [26] S. Y. Choi, K. Hagiwara and M. S. Baek, *Phys. Rev. D* **54** (1996) 6703 [hep-ph/9605334].
- [27] G. J. Gounaris, J. Layssac and F. M. Renard, *Z. Phys. C* **69** (1996) 505 [hep-ph/9505430].
- [28] O. Nachtmann, F. Nagel, M. Pospischil and A. Utermann, “Effective-Lagrangian approach to  $\gamma\gamma \rightarrow WW$ ; II: Results and comparison with  $e^+e^- \rightarrow WW$ ,” hep-ph/0508133.
- [29] D. Atwood and A. Soni, *Phys. Rev. D* **45**, 2405 (1992);  
M. Davier, L. Duflot, F. Le Diberder and A. Roug e, *Phys. Lett. B* **306**, 411 (1993).
- [30] O. Nachtmann and F. Nagel, *Eur. Phys. J. C* **40** (2005) 497 [hep-ph/0407224].
- [31] O. Nachtmann, “Elementary Particle Physics: Concepts and Phenomena,” Springer Verlag, Berlin, Germany (1990).